



Cite this: *Chem. Commun.*, 2014, 50, 13687

Received 20th July 2014,
Accepted 16th September 2014

DOI: 10.1039/c4cc05606j

www.rsc.org/chemcomm

Evidence for covalent bonding of aryl groups to MnO₂ nanorods from diazonium-based grafting†

K. J. Bell, P. A. Brooksby, M. I. J. Polson and A. J. Downard*

We show here that the surface of MnO₂ nanorods can be modified with aryl groups by grafting from aqueous and non-aqueous solutions of aryldiazonium salts. X-ray photoelectron spectroscopy provides direct evidence for covalent bonding of aryl groups to MnO₂ through surface oxygens.

Manganese dioxide, especially in nanostructured forms, is a technologically important material that holds promise as an inexpensive and environmentally friendly candidate for advanced applications in energy storage,¹ sensing² and catalysis.³ A key feature of these applications is their reliance on reactions or interactions at the MnO₂ surface; manipulation of surface properties is hence important for optimised performance. For example, mechanical and chemical stability, hydrophobic/hydrophilic balance and capacitance are influenced by the nature of the surface. Covalently anchoring selected species through chemical grafting can modify surface properties and also enables new device architectures and the attachment of additional active components after further coupling reactions.⁴ Generation of aryl radicals from aryldiazonium ions is a versatile and well-studied grafting method.⁴ Radical attack at the substrate results in a covalent bond between the aryl group and the surface. This strategy has been used to produce stable organic layers and molecular tethers on a wide variety of surfaces.⁴

Through the diazonium ion grafting route, organic layers have been deposited on oxides of Cu,⁵ Si,⁶ Fe,⁷ Ti,^{6b,8} Al,^{5,6b,9} Cr,¹⁰ In (in the form of indium tin oxide),¹¹ V¹² (in the form of Li_{1.1}V₃O₈) and Gd.^{6b} X-ray photoelectron spectroscopy (XPS) characterisation of modified Cu surfaces revealed bonding between surface O atoms and aryl groups and more tentatively, bonding between surface Cu atoms and aryl groups.⁵ Similarly, time-of-flight secondary-ion mass spectrometry (TOF-SIMS) of

modified Al nanoparticles demonstrated that aryl groups are bound to the surface, mainly through Al–O–C linkages.⁹ For other oxides, it has been assumed that the organic layer is covalently attached however there is increasing evidence that physisorbed layers can be deposited from aryldiazonium salt solutions¹³ and hence the nature of the interaction between the layer and the surface requires careful investigation.

In this work we demonstrate the modification of MnO₂ nanorods by grafting from aryldiazonium salt solutions and we provide evidence for covalent bonding between the aryl layer and the nanorod surface.

MnO₂ nanoparticles were synthesised by a solution method¹⁴ and aged for a week at 60 °C (see ESI† for details). Analysis by scanning electron microscopy (SEM) showed predominantly nanorod structures, ~150 nm long and with diameter ~20 nm (Fig. S1a, ESI†). The X-ray diffraction (XRD) pattern (Fig. S2a, ESI†) indicates a α -MnO₂ (cryptomelane) structure.¹⁴ A typical cyclic voltammogram (CV) obtained in 0.1 M KCl of a glassy carbon (GC) electrode (3 mm diameter) drop-coated with nanorods (5 μ L of a 2 mg mL⁻¹ solution) is shown in Fig. 1, scan a. The CV, which is similar to those previously reported,¹⁵ shows a quasi-rectangular response typical of pseudocapacitance overlaid

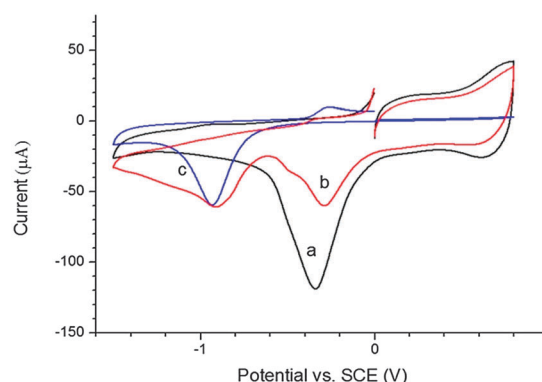


Fig. 1 CVs in 0.1 M KCl, 1:9 ethanol:water of: (a) as-prepared MnO₂; (b) NP-MnO₂ and (c) NP-GC. Scan rate = 50 mV s⁻¹.

MacDiarmid Institute for Advanced Materials and Nanotechnology,
Department of Chemistry, University of Canterbury, Private Bag 4800,
Christchurch 8140, New Zealand. E-mail: alison.downard@canterbury.ac.nz

† Electronic supplementary information (ESI) available: Experimental details, Fig. S1–S5. See DOI: 10.1039/c4cc05606j

with peaks that are attributed to the (de)intercalation of H^+ and K^+ ions.¹⁶

Two strategies were developed for modification of MnO_2 nanorods using diazonium ion chemistry: modification in basic aqueous medium, and in acetonitrile (ACN). The more usual acidic conditions could not be employed owing to the ease of reduction of MnO_2 at low pH, giving soluble $Mn(II)$ species.

4-Nitrobenzenediazonium tetrafluoroborate (NBD) was chosen for proof-of-concept experiments in basic medium because the presence of grafted nitrophenyl (NP) groups can be conveniently detected electrochemically. In basic conditions, an aryldiazonium ion forms the corresponding diazoate which decomposes *via* a homolytic bond cleavage to give an aryl radical.¹⁷ NBD (50 mM final concentration) was added to a suspension of MnO_2 nanorods (2 mg mL^{-1}) in 0.1 M NaOH and the mixture was sonicated for 1 h. After washing using repeated cycles of centrifugation and sonication in ethanol and ultrapure water, the solid was dried under vacuum. SEM imaging and XRD analysis (Fig. S1b, c and S2b, c, ESI,† respectively) of the modified sample, and of a 'NaOH blank' (MnO_2 nanorods sonicated in 0.1 M NaOH for 1 h) confirmed that the nanorod morphology and crystal structure were unchanged after these treatments.

Fig. 1, scan b, shows the CV obtained at a GC electrode drop-coated with $5\text{ }\mu\text{L}$ of a 2 mg mL^{-1} solution of NP-modified MnO_2 (NP- MnO_2). For comparison, scan c was obtained under the same conditions at a GC electrode modified with an NP film, grafted by electroreduction of NBD (NP-GC). The CVs provide clear evidence for the presence of NP groups in the modified MnO_2 sample. The irreversible peak at $E_{pc} = -0.9\text{ V}$ is attributed to reduction of NP groups;¹⁸ as expected it closely corresponds to the same process in NP-GC (scan c) but is absent in unmodified MnO_2 (scan a).

Thermogravimetric analysis (TGA) of MnO_2 and NP- MnO_2 samples further supports the presence of NP groups after reaction with NBD. The samples were heated at a rate of $2\text{ }^\circ\text{C min}^{-1}$ under an N_2 atmosphere. The mass-loss profile for MnO_2 (NaOH blank) (Fig. 2 curve a) is similar to that previously reported for α - MnO_2 and shows the gradual loss of surface and structural water up to $\sim 550\text{ }^\circ\text{C}$, after which a sharp decrease in mass corresponds to a phase transition from α - MnO_2 to Mn_2O_3 with the release of oxygen.¹⁹ An additional $4 \pm 2\%$ ($n = 4$) mass-loss

between 200 and $330\text{ }^\circ\text{C}$ is seen for NP- MnO_2 (Fig. 2 curve b) consistent with additional volatile components and hence the presence of NP groups. This behaviour can be compared with that reported by Toupin and Bélanger for carbon black modified with NP groups through reaction with the corresponding diazonium salt.²⁰ Using mass spectrometry coupled with TGA they observed loss of NO between 150 and $250\text{ }^\circ\text{C}$ and the simultaneous release of NO, NO_2 and CO_2 between 350 and $600\text{ }^\circ\text{C}$. Release of NO and NO_2 originates in the decomposition of NP groups, and CO_2 (also observed for unmodified carbon black) from loss of lactones on the carbon surface. For NP- MnO_2 samples, the additional mass loss (over that for the unmodified samples) is essentially complete at $330\text{ }^\circ\text{C}$ suggesting that loss of NP groups is complete by this temperature. Catalytic decomposition of NP groups by the MnO_2 substrate is a likely explanation. Supporting this proposal, Suib and co-workers found that catalytic decomposition of aromatic hydrocarbons adsorbed to several MnO_2 materials occurred over a wide temperature range in an Ar atmosphere, with the major product evolution seen between $200\text{--}400\text{ }^\circ\text{C}$.^{3b}

The effectiveness of non-aqueous conditions for modification of MnO_2 nanorods was investigated using 4-aminobenzenediazonium ion (ABD) prepared *in situ*. This derivative was used to demonstrate that the reaction is not limited to NBD and also because aminophenyl (AP) groups are useful molecular tethers. *tert*-Butyl nitrite (50 mM final concentration) was added to an equimolar ACN solution of 1,4-diaminobenzene (AMB) containing MnO_2 nanorods (2 mg mL^{-1}). After sonicating for 1 h, the solid was washed with repeated cycles of sonication and centrifugation, using alternatively, ethanol and ultrapure water, followed by drying under vacuum. In this strategy, modification of MnO_2 with AP groups is expected to occur if an active modifier (the aryl radical or cation) forms spontaneously,²¹ or *via* reduction of ABD by MnO_2 .²²

SEM imaging and XRD analysis (Fig. S1d, e and S2d, e, ESI,† respectively) of the modified sample, and of an 'ACN blank' (MnO_2 nanorods sonicated in 50 mM *tert*-butyl nitrite in ACN for 1 h) confirmed there was no change in nanorod morphology or crystal structure after reaction with AMB. The treated sample was examined by TGA (Fig. 2) showing a gradual $6.6 \pm 0.4\%$ ($n = 3$) mass loss between $\sim 200\text{--}500\text{ }^\circ\text{C}$ that is absent in the blank. Similar behaviour was observed for AP-modified carbon powder²² suggesting that the MnO_2 nanorods have been modified with an AP film.

NP- MnO_2 and AP- MnO_2 samples were further analysed using XPS. Survey scans of the samples and corresponding blanks (Fig. S3, ESI†) gave the elemental compositions listed in Table 1. As expected, N is present in the modified samples but absent in the blanks, and both modified samples have significantly greater atomic %C than the corresponding blanks. (Carbon in the blanks and as-prepared MnO_2 is assumed to result from contamination during measurement.) The ratio of atomic% (K + Na): Mn varies widely between samples. For AP- MnO_2 and the ACN blank, the ratio matches that expected for cryptomelane (chemical composition KMn_8O_{16}). In contrast, after treatment in basic reaction conditions the NP- MnO_2 and NaOH blank samples have significantly increased fractions of Na giving (K + Na): Mn ratios of 0.46 and 0.39 respectively. This increase

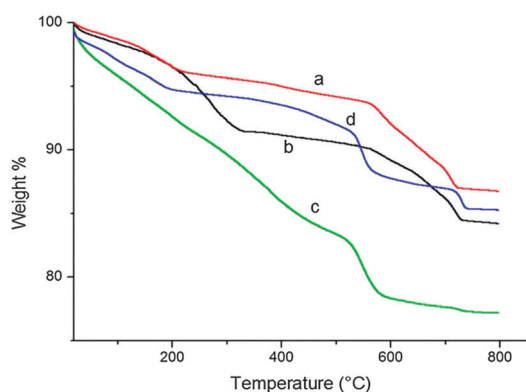


Fig. 2 TGA curves of: (a) MnO_2 (NaOH blank), (b) NP- MnO_2 , (c) AP- MnO_2 and (d) MnO_2 (ACN blank).

Table 1 XPS atomic percent and average oxidation state (AOS) data for MnO₂ nanorods

MnO ₂ sample	At%						C ⁺ :Mn ^a	AOS	AOS error
	Mn	O	C	N	K	Na			
NaOH blank	21.3	53.2	17.2	—	3.2	5.1	0.39	3.992 ^b	0.005 ^d
NP-MnO ₂	17.3	47.9	23.7	3.1	2.6	5.3	0.46	3.97 ^c	0.07 ^e
ACN blank	24.4	55.6	16.8	—	3.2	0.13	3.86 ^b	3.86 ^b	0.04 ^d
AP-MnO ₂	21.6	56.1	18.1	1.5	2.8	0.13	0.13	3.65 ^c	0.07 ^e

^a C⁺ is the number of charge-balancing cations (Na⁺ and K⁺). ^b AOS measurement from potentiometric titration. ^c AOS measurement from XPS splitting data. ^d Standard error of mean (3 samples). ^e Standard error of the regression.

in Na content could be due to a simple replacement of charge-compensating H⁺ by Na⁺ or alternatively could indicate a decrease in the average oxidation state of MnO₂ after exposure to basic conditions. The latter possibility was investigated by determining the average oxidation states (AOS) of the materials (see ESI,† Experimental and Fig. S4).

The data in Table 1 show that NP-MnO₂ and the NaOH blank samples have AOS close to the expected value of 4 and there is no evidence that modification with NP groups or treatment in basic conditions affects the AOS. This suggests that the observed increase in Na⁺ after immersion in NaOH is due to replacement of H⁺ by Na⁺. On the other hand, the AP-MnO₂ sample which was modified in ACN has a significantly lower AOS. Although the mean AOS for the ACN blank sample is also lower, it is not significantly different to the NP-MnO₂ sample and hence it is unclear whether it is the grafted AP groups or the reaction solvent that leads to the decrease in AOS. This is a question for further investigation.

XPS narrow scans of the C 1s, N 1s, O 1s and Mn 2p regions were analysed to investigate the bonding between modifying groups and MnO₂. All samples show the expected O 1s peaks for Mn–O–Mn, M–OH and H–O–H²³ at ~530, 531 and 532 eV, respectively (Fig. 3a–d). However NP-MnO₂ and AP-MnO₂ have an additional peak at ~533 eV. This binding energy is in the region expected for O in metal–O–C bonds^{5,24} but also for O in the NO₂ group of NP.²⁵ However, the presence of the peak in AP-MnO₂ which does not contain the NO₂ group confirms that aryl groups are covalently attached to the nanorod surface through Mn–O–C bonds. The N 1s spectra for the modified samples (Fig. 3e and g) have a peak at ~400 eV assigned to amine (for AP-MnO₂) and azo groups (NP-MnO₂ and AP-MnO₂);¹⁸ NP-MnO₂ also shows the expected peak at ~406 eV assigned to the N in NO₂ groups.¹⁸ (The absence of this peak in AP-MnO₂ confirms that there are no NO₂ groups and hence that the O 1s peak at ~533 eV for this sample must be due to Mn–O–C bonding.) Adventitious carbon complicates the C 1s scans (Fig. S5a–e, ESI†) preventing assignment of peaks and similarly the large amount of multiplet splitting present in the Mn 2p region (Fig. S5f–j, ESI†) prevents detection of any small changes in the Mn signal after modification.

We have demonstrated covalent modification of MnO₂ nanorods using diazonium ions under two conditions: using an isolated diazonium salt in 0.1 M NaOH and through *in situ* formation of the diazonium ion in ACN solution. XPS studies give direct evidence that aryl groups are attached to the nanorod surface *via* Mn–O–C bonds however the possible involvement of Mn–C bonds cannot be discounted. The stable attachment of aryl groups opens many opportunities for enhancing the performance of MnO₂ materials through tuning the surface properties. Applications of these modified materials are under investigation in ongoing work.

Notes and references

- (a) Q. Lu, J. G. Chen and J. Q. Xiao, *Angew. Chem., Int. Ed.*, 2013, **52**, 1882; (b) H. Manjunatha, G. S. Suresh and T. V. Venkatesha, *J. Solid State Electrochem.*, 2011, **15**, 431.
- (a) S. Ling, R. Yuan, Y. Chai and T. Zhang, *Bioprocess Biosyst. Eng.*, 2009, **32**, 407; (b) R. Yamaguchi, A. Sato, S. Iwai, K. Tomono and M. Nakayama, *Electrochem. Commun.*, 2013, **29**, 55.
- (a) T. Takashima, K. Hashimoto and R. Nakamura, *J. Am. Chem. Soc.*, 2012, **134**, 1519; (b) H. C. Genuino, S. Dharmarathna, E. C. Njagi, M. C. Mei and S. L. Suib, *J. Phys. Chem. C*, 2012, **116**, 12066; (c) C. D. Lokhande, D. P. Dubal and O. S. Joo, *Curr. Appl. Phys.*, 2011, **11**, 255.
- D. Bélanger and J. Pinson, *Chem. Soc. Rev.*, 2011, **40**, 3995.
- B. L. Hurley and R. L. McCreery, *J. Electrochem. Soc.*, 2004, **151**, B252.
- (a) N. Griffete, J. F. Dechezelles and F. Scheffold, *Chem. Commun.*, 2012, **48**, 11364; (b) J. F. Dechezelles, N. Griffete, H. Dietsch and F. Scheffold, *Part. Part. Syst. Charact.*, 2013, **30**, 579.
- N. Griffete, F. Herbst, J. Pinson, S. Ammar and C. Mangeney, *J. Am. Chem. Soc.*, 2011, **133**, 1646.
- A. Merson, T. Dittrich, Y. Zidon, J. Rappich and Y. Shapira, *Appl. Phys. Lett.*, 2004, **85**, 1075.
- Y. A. Atmane, L. Sicard, A. Lamouri, J. Pinson, M. Sicard, C. Masson, S. Nowak, P. Decorse, J. Y. Piquemal, A. Galtayries and C. Mangeney, *J. Phys. Chem. C*, 2013, **117**, 26000.
- M. Hinge, M. Ceccato, P. Kingshott, F. Besenbacher, S. U. Pedersen and K. Daasbjerg, *New J. Chem.*, 2009, **33**, 2405.
- S. Maldonado, T. J. Smith, R. D. Williams, S. Morin, E. Barton and K. J. Stevenson, *Langmuir*, 2006, **22**, 2884.
- F. Tanguy, J. Gaubicher, A. C. Gaillot, D. Guyomard and J. Pinson, *J. Mater. Chem.*, 2009, **19**, 4771.

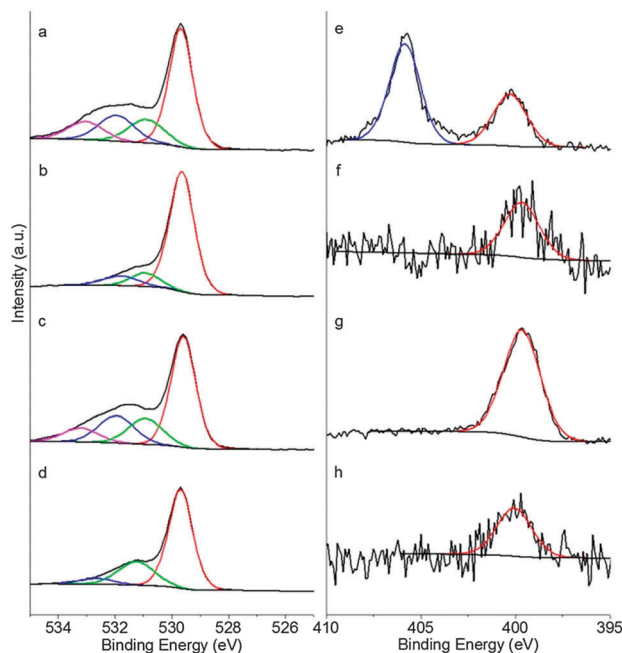


Fig. 3 XPS narrow scans: O 1s (a–d) and N 1s (e–h) for NP-MnO₂ (a, e), NaOH blank (b, f), AP-MnO₂ (c, g) and ACN Blank (d, h).

- 13 (a) H. F. Ma, L. Lee, P. A. Brooksby, S. A. Brown, S. J. Fraser, K. C. Gordon, Y. R. Leroux, P. Hapiot and A. J. Downard, *J. Phys. Chem. C*, 2014, **118**, 5820; (b) B. Cui, J. Y. Gu, T. Chen, H. J. Yan, D. Wang and L. J. Wan, *Langmuir*, 2013, **29**, 2955; (c) D. R. Jayasundara, R. J. Cullen and P. E. Colavita, *Chem. Mater.*, 2013, **25**, 1144.
- 14 D. Portehault, S. Cassaignon, E. Baudrin and J. P. Jolivet, *J. Mater. Chem.*, 2009, **19**, 2407.
- 15 T. Brousse, M. Toupin, R. Dugas, L. Athouel, O. Crosnier and D. Bélanger, *J. Electrochem. Soc.*, 2006, **153**, A2171.
- 16 (a) H. Kanoh, W. P. Tang, Y. Makita and K. Ooi, *Langmuir*, 1997, **13**, 6845; (b) O. Ghodbane, F. Ataherian, N. L. Wu and F. Favier, *J. Power Sources*, 2012, **206**, 454.
- 17 (a) F. I. Podvorica, F. Kanoufi, J. Pinson and C. Combella, *Electrochim. Acta*, 2009, **54**, 2164; (b) A. Sienkiewicz, M. Szymula, J. Narkiewicz-Michalek and C. Bravo-Diaz, *J. Phys. Org. Chem.*, 2014, **27**, 284.
- 18 S. S. Yu, E. S. Tan, R. T. Jane and A. J. Downard, *Langmuir*, 2007, **23**, 11074.
- 19 W. M. Dose and S. W. Donne, *Mater. Sci. Eng., B*, 2011, **176**, 1169.
- 20 M. Toupin and D. Bélanger, *J. Phys. Chem. C*, 2007, **111**, 5394.
- 21 B. M. Simons, J. Lehr, D. J. Garrett and A. J. Downard, *Langmuir*, 2014, **30**, 4989.
- 22 J. Lyskawa, A. Grondein and D. Bélanger, *Carbon*, 2010, **48**, 1271.
- 23 B. Djurfors, J. N. Broughton, M. J. Brett and D. G. Ivey, *Acta Mater.*, 2005, **53**, 957.
- 24 (a) S. Akhter, X. L. Zhou and J. M. White, *Appl. Surf. Sci.*, 1989, **37**, 201; (b) C. Dicke, M. Morstein and G. Hahner, *Langmuir*, 2002, **18**, 336.
- 25 K. Roodenko, M. Gensch, J. Rappich, K. Hinrichs, N. Esser and R. Hunger, *J. Phys. Chem. B*, 2007, **111**, 7541.